

Supplemental Figure 1. ERK2 expression is abolished in neural progenitor cells beginning at E13.5. **A-B**, Expression of hGFAP-cre activity. Sagittal sections of adult hGFAP-cre;R26R mice were stained for X-gal and counterstained with neutral red. High magnification inset in **B** demonstrates the extent of recombination throughout the cortex. **C**, ERK2 expression in ERK2 CKO and wild-type mice at P2. Coronal sections of ERK2 CKO (left) and wild type littermates (right) were immunostained with an ERK2 specific antibody and visualized using DAB. **D-I**, Coronal sections of P2 ERK2 CKO and wild-type mice immunostained with an ERK2 specific antibody (red) and colabeled with antibodies directed to **(D-E)** Tbr1, the preplate/layer VIb marker (green), **(F-G)** GABAergic interneuron marker, GABA (green) and **(H-I)** Reelin (green) which labels Cajal-Retzius cells. The merged images and inset enlargements are shown in the far left panels of each.

Supplemental Figure 2. ERK2 expression is reduced in the hippocampus, but not the amygdala in ERK2 CKO mice. **A-B**, ERK2 expression was assessed by immunostaining with an anti-ERK2 specific antibody. Corresponding coronal sections of adult ERK2 CKO (**A**) and littermate wild-types (**B**) were evaluated for ERK2 expression in the hippocampus and amygdala. Note that ERK2 is most highly expressed in the dentate gyrus (DG) and CA3 regions of the hippocampus and was lost in these areas in the mutant mice. No change in ERK2 expression was identified within the basolateral amygdala (B/LA).

Supplemental Figure 3. The ERK2 CKO cortex does not exhibit apoptosis. Analysis of apoptosis was performed by immunostaining with anti-Caspase 3 antibody (**A**, DAB) and TUNEL staining (**B**, green). Corresponding coronal sections from E17 ERK2 CKO (left) and wildtype (right) brains were stained with anti-Caspase 3 antibodies (note black arrow) and by TUNEL staining (white arrow).

Supplemental Figure 4. The number of Pax6 and Tbr2 immunoreactive cells at E14.5 is not altered by conditional inactivation of ERK2. Cellular analysis was performed by immunohistochemistry of E14.5 cryosections with anti-Pax6 (red) and anti-Tbr2 (green) antibodies and counting of immunoreactive cells for each marker and for those cells expressing both markers. Two-way ANOVA, $p > 0.05$ for each.

Supplemental Figure 5. Patients with deletions of distal 22q11 have reduced ERK2 levels. **A**, Schematic representation of Chromosome 22q11 with the centromere (CEN) to the left and telomeric (TEL) end to the right. Low copy repeats, LCRs are denoted by black boxes. The gene encoding CRKL is located between LCR-C and LCR-D and is included in the common 3Mb DiGeorge Syndrome deletion spanning from LCR-A to LCR-D. The *MAPK1* gene is located between LCR-D and LCR-E and is included in a 1 Mb distal 22q11 deletion occurring between these two LCRs. The D-E deletion interval is expanded to illustrate the other genes located within this 1Mb region. **B**, Lymphoblasts from normal subjects, distal 22q11 deletion patients, and DiGeorge Syndrome patients were lysed and prepared for Western blot analysis. The levels of ERK1, ERK2, and

CRKL were detected by immunoblotting and representative blots are shown. G3PDH levels were assayed for loading controls. **C**, Quantification of ERK2 levels from normal, D-E deletion, and DiGeorge Syndrome patient lymphoblasts (normal, n=4, D-E, n=2, DiGeorge, n=1, p=0.0026).

Supplemental Table 1 and 2. Inactivation of ERK2 does not alter the morphology of cortical neurons.

Table 1- Parameters of basal dendrites of layer III pyramidal neurons

Order	Quantity		Length (μm)		Surface area (μm^2)		Volume (μm^3)	
	CKO	WT	CKO	WT	CKO	WT	CKO	WT
1	47.67 \pm 1.76	60.67 \pm 5.69	122.72 \pm 9.80	156.52 \pm 2.62	910.44 \pm 101.61	1141.69 \pm 25.23	568.08 \pm 92.88	762.00 \pm 29.85
2	47.33 \pm 4.67	59.67 \pm 3.48	148.30 \pm 6.51	153.82 \pm 4.44	1085.68 \pm 75.67	901.99 \pm 48.78	660.29 \pm 71.69	515.32 \pm 32.39
3	38.00 \pm 1.15	25.67 \pm 0.33 *	158.15 \pm 3.65	135.16 \pm 6.58	1021.18 \pm 42.84	781.59 \pm 30.18 *	528.76 \pm 18.40	402.61 \pm 22.79 *

Mean values \pm SEM.

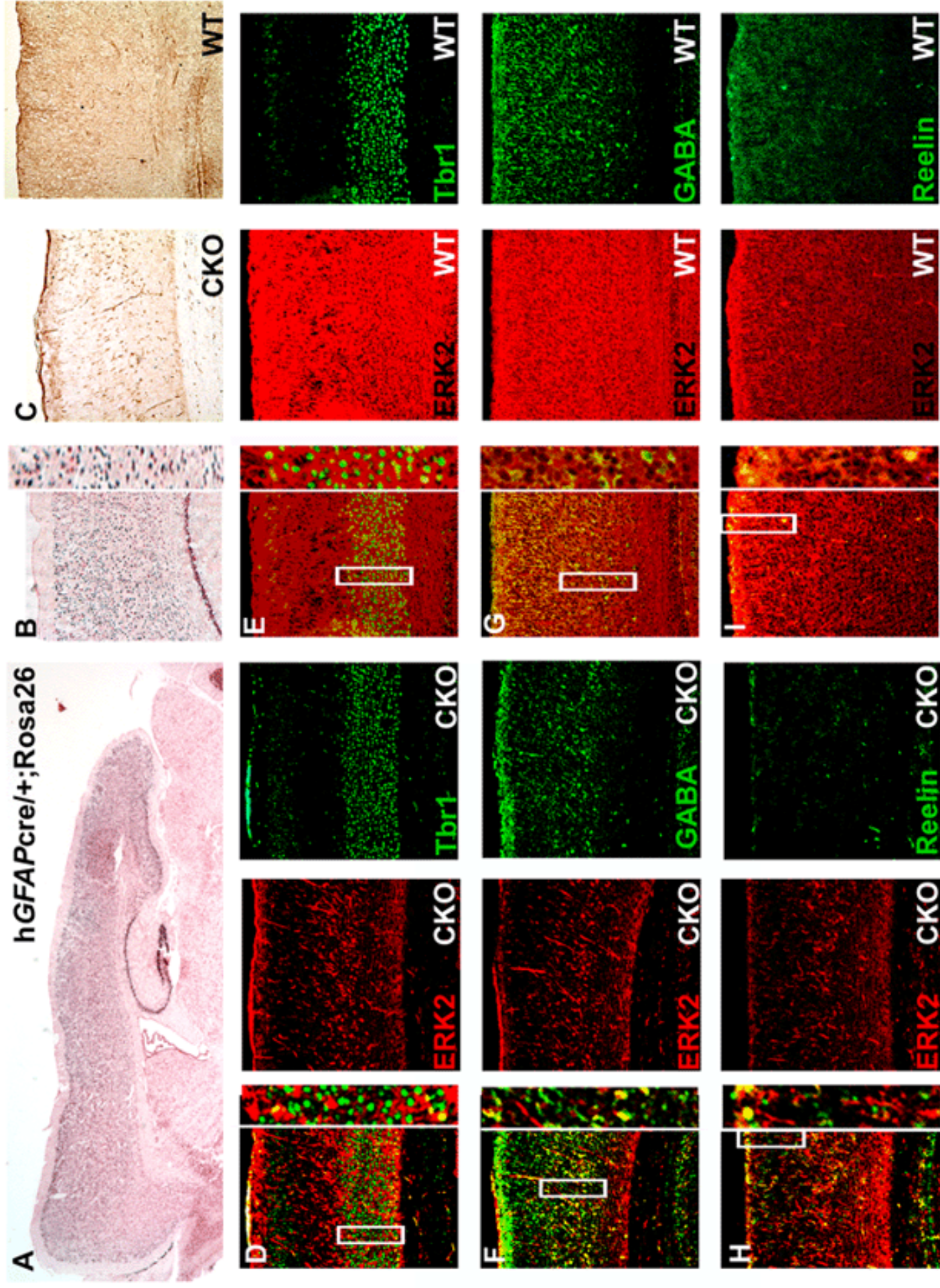
* P< 0.05.

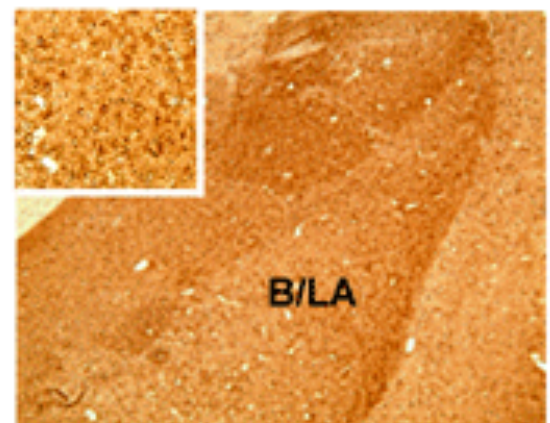
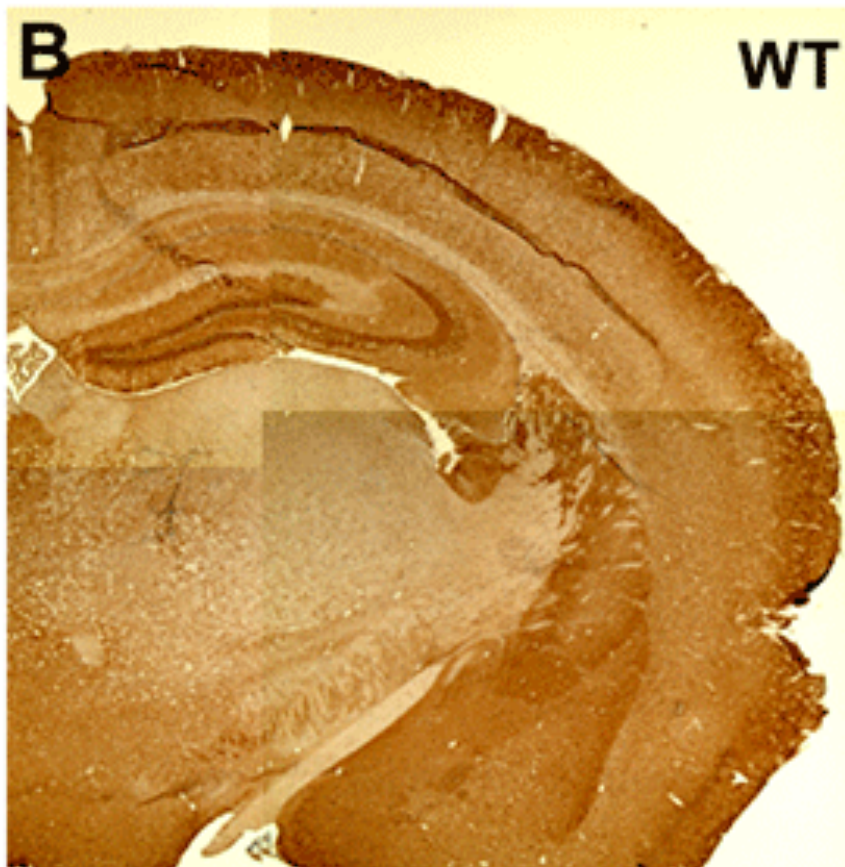
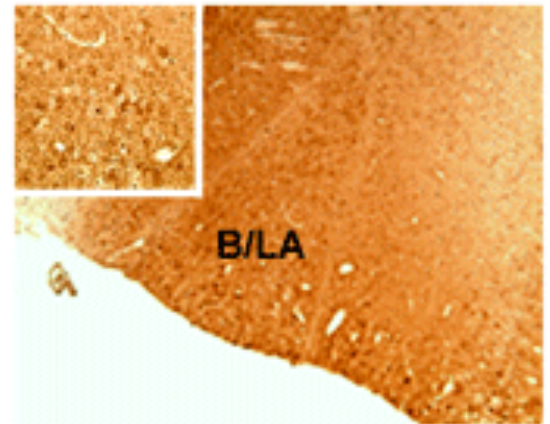
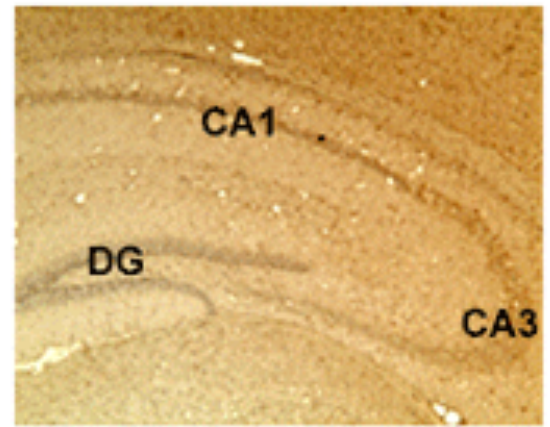
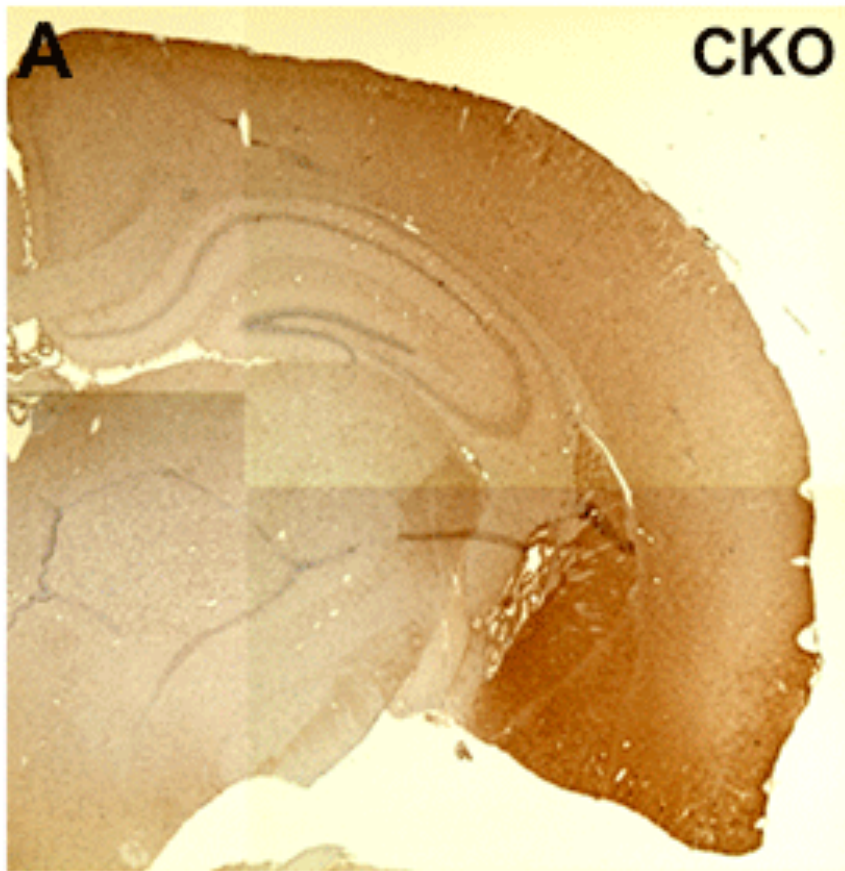
Table 2- Parameters of basal dendrites of Layer V pyramidal neurons

Order	Quantity		Length (μm)		Surface area (μm^2)		Volume (μm^3)	
	CKO	WT	CKO	WT	CKO	WT	CKO	WT
1	42.67 \pm 5.90	61.67 \pm 1.76	132.53 \pm 24.96	156.30 \pm 26.47	1238.69 \pm 272.60	1151.01 \pm 279.62	994.20 \pm 228.48	728.64 \pm 199.65
2	41.67 \pm 5.49	42.33 \pm 3.93	142.68 \pm 32.83	169.34 \pm 31.41	1246.00 \pm 339.24	1323.47 \pm 310.27	922.62 \pm 260.06	882.67 \pm 219.33
3	14.00 \pm 1.15	18.33 \pm 1.20	149.35 \pm 22.53	181.39 \pm 37.52	1516.03 \pm 96.15	1409.52 \pm 328.76	978.03 \pm 161.41	905.58 \pm 219.87

Mean values \pm SEM.

* $P < 0.05$.

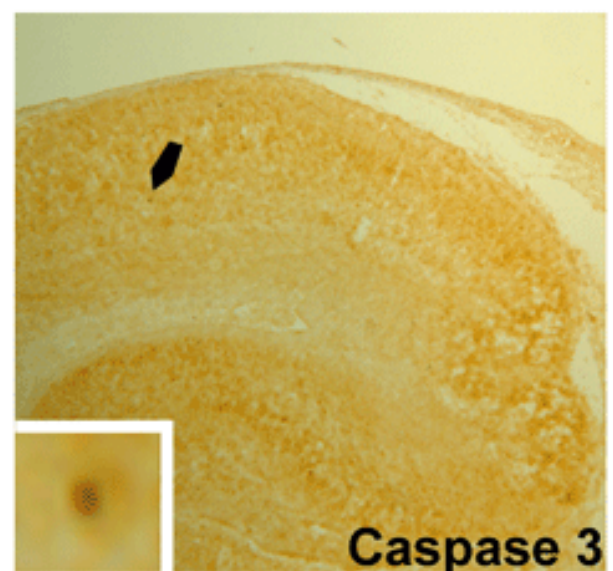
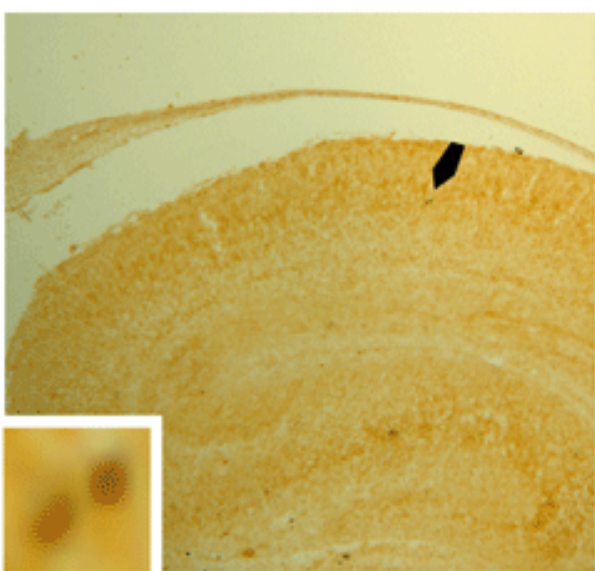




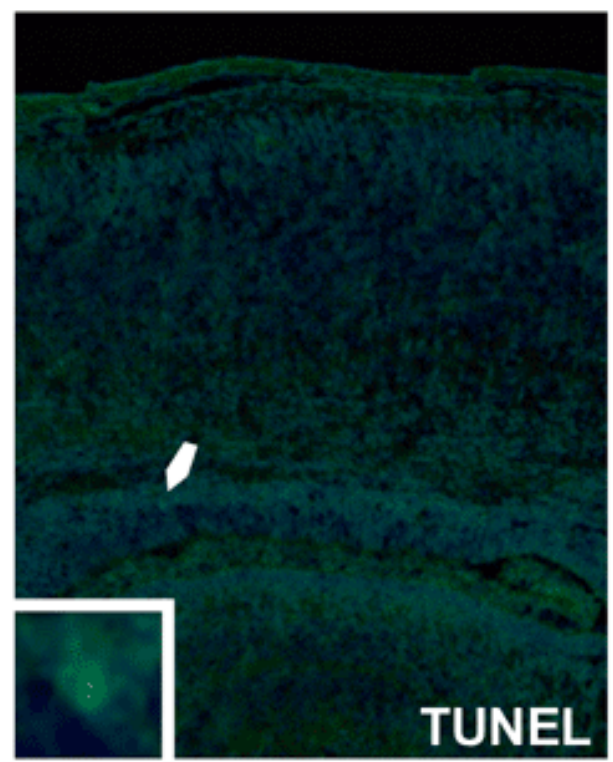
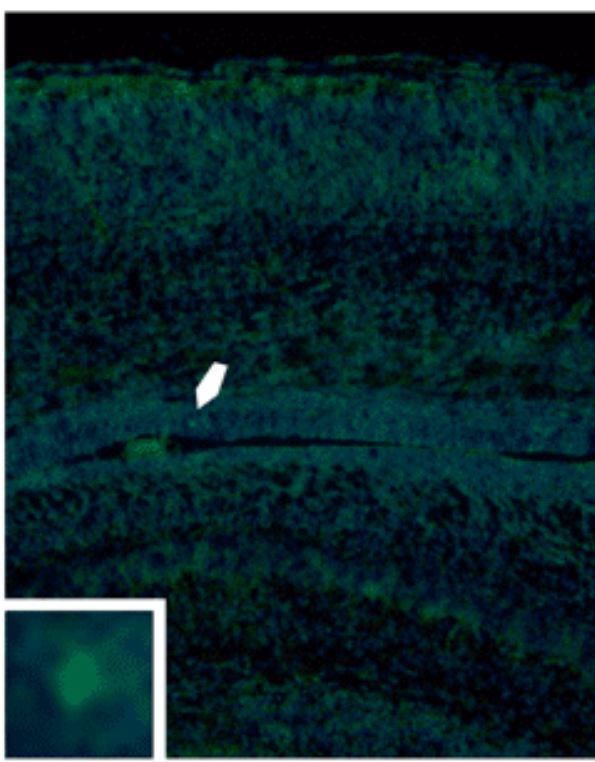
CKO

WT

A



B



CKO**WT**